

A major purpose of the Technical Information Center is to provide the broadest dissemination possible of information contained in DOE's Research and Development Reports to business, industry, the academic community, and federal, state and local governments.

Although a small portion of this report is not reproducible, it is being made available to expedite the availability of information on the research discussed herein.

CONF-850414--1

Los Alamos National Laboratory is operated by the University of California for the United States Department of Energy under contract W-7405-ENG-32

Study of Rare Muon Decay Modes with the Crystal Box*

TITLE:

AUTHOR(S)

V. Sandberg, R.D. Bolton, J.D. Bowman, R.D. Carlini, M.D. Cooper, M.
Doug-Van, J.S. Frank, A.L. Hallin, P. Heusi, C.M. Hoffman, G.E. Hogan, F.B.
Marlam, H.S. Matis, R.E. Mischke, D.E. Nagle, G.H. Sanders, U. Sennhauser, R.L.
Telaga, R.W. Werbeck, R.A. Williams
Los Alamos National Laboratory
Los Alamos, NM 87545

SUBMITTED TO

D.P. Grosnick, S.C. Wright
University of Chicago
Chicago, Illinois

LA-UR--85-2346

DE85 015678

S.L. Wilson, E.B. Hughes, R. Hofstadter
Hansen Laboratory, Stanford University
Stanford, California

J. McDonough, V.L. Highland
Temple University
Philadelphia, Pennsylvania

Text of an invited talk presented at the Washington Meeting of the American
Physical Society, Division of Nuclear Physics, 24-27 April, 1985, held in
Crystal City, Virginia

By acceptance of this article, the publisher recognizes that the U.S. Government retains a nonexclusive, royalty-free license to publish or reproduce
the published form of this contribution or to allow others to do so, for U.S. Government purposes.

The Los Alamos National Laboratory requests that the publisher identify this article as work performed under the auspices of the U.S. Department of Energy.

 DISTRIBUTION OF THIS DOCUMENT IS UNLIMITED

 **Los Alamos** Los Alamos National Laboratory
Los Alamos, New Mexico 87545

Study of Rare Muon Decay Modes with the Crystal Box*

**V. Sandberg, R.D. Bolton, J.D. Bowman, R.d. Carlini, M.D. Cooper, M.
Doung-Van, J.S. Frank, A.L. Hallin, P. Heusi, C.M. Hoffman, G.E.
Hogan, F.G. Marlam, H.S. Matis, R.E. Mischke, D.E. Nagle, G.H. Sanders,
U. Sennhauser, R.L. Talaga, R.W. Werbeck, R.A. Williams
Los Alamos National Laboratory
Los Alamos, NM 87545**

**D.P. Grosnick, S.C. Wright
University of Chicago
Chicago, Illinois**

**S.L. Wilson, E.B. Hughes, R. Hofstadter
Hansen Laboratory, Stanford University
Stanford, California**

**J. McDonough, V.L. Highland
Temple University
Philadelphia, Pennsylvania**

**Text of an invited talk presented at the Washington Meeting of the
American Physical Society, Division of Nuclear Physics, 24-27
April, 1985, held in Crystal City, Virginia**

***Supported by the U.S. Department of Energy**

Abstract

We report on a search for the lepton family-number-nonconserving decays $\mu^+ \rightarrow e^+ e^- e^+$, $\mu^+ \rightarrow e^+ \gamma$, and $\mu^+ \rightarrow e^+ \gamma \gamma$, using the Crystal Box detector at LAMPF. The experiment was run in the stopped muon channel at LAMPF during the winter and summer of 1984. Muons were stopped in the middle of a detector system consisting of a cylindrical drift chamber, a plastic scintillator hodoscope, and a segmented array of sodium iodide crystals. The sodium iodide surrounded the hodoscope and drift chamber. Events consistent with any of the above decays were recorded. The off-line data analysis imposed requirements on the timing, vertex location, and energy and momentum conservation for each event. Radioactive sources, conventional muon decay spectra, and photons from the process $\pi^- p \rightarrow n \gamma$ and $\pi^- p \rightarrow n \pi^0$ were used to provide energy calibration and resolution estimates. The inner bremsstrahlung processes $\mu^+ \rightarrow e^+ \gamma \gamma$ and $\mu^+ \rightarrow e^+ e^- e^+ \gamma$ were observed at the expected rates. Details of the detector, the data analysis, and our latest bounds for the branching ratios will be presented.

DISCLAIMER

This report was prepared as an account of work sponsored by an agency of the United States Government. Neither the United States Government nor any agency thereof, nor any of their employees, makes any warranty, express or implied, or assumes any legal liability or responsibility for the accuracy, completeness, or usefulness of any information, apparatus, product, or process disclosed, or represents that its use would not infringe privately owned rights. Reference herein to any specific commercial product, process, or service by trade name, trademark, manufacturer, or otherwise does not necessarily constitute or imply its endorsement, recommendation, or favoring by the United States Government or any agency thereof. The views and opinions of authors expressed herein do not necessarily state or reflect those of the United States Government or any agency thereof.

It is my pleasure to present to you, today, some preliminary results on a search for rare muon decays carried out at LAMPF. The experiment ran during the winter and summer 1984 cycles of the LAMPF calendar with a detector called the Crystal Box. The name of the detector was derived from the large number of sodium iodide detectors used in the experiment. This appears to be a case of carrying crystals to Crystal City.

We looked for the lepton-family-nonconserving decays of a muon into an electron and a photon and for the three-body decays of a muon into an electron and two photons or into three electrons. The experiment was mounted by a collaboration of physicists from Los Alamos National Laboratory, University of Chicago, Stanford University, and Temple University (fig. 1).

To place the experiment in context and to explain why the effort was undertaken I would like to briefly comment on the "Standard Model" (fig. 2). The "Standard Model" groups the leptons into three families. By construction it conserves the additive lepton family numbers associated with these groupings. Furthermore, the various interactions described by the "Standard Model" do not mediate lepton-family number-changing processes. As a fundamental theory of the world the "Standard Model" is consistent, but incomplete. Various extensions that can produce our studied transitions have been proposed, for example the existence of massive neutrinos and neutrino oscillations, modifications of the Higgs sector of the theory, and enlargements of the gauge group as in grand unified theories and supersymmetric theories. Different extensions predict different rates for each of the muon rare-decay modes. It is, therefore, important to search for all three modes. In this way the proposed extensions may be compared with the experimental limits and judged accordingly.

The study of the decay modes of the muon began in 1947 with the availability of muon beams from the postwar accelerators. There has been a steady history of improvement in experiments searching for these decays as shown in fig. 3. No lepton-family number-nonconserving decay has been seen. The 90% confidence level limits on the branching ratios for these decays prior to this experiment are shown in fig. 4. It is interesting to note that the limits for the three modes $\mu \rightarrow e \gamma$, $\mu \rightarrow e e \gamma$, and $\mu \rightarrow e e e$ were established at the three "meson factories" LAMPF, TRIUMF, and SIN, respectively.

An experiment sensitive to a branching ratio of the order 10^{-10}

requires a sample of approximately 10^{11} muon decays (fig. 5). The long lifetime of the muon (2.2×10^{-6} second) makes it necessary to use stopped muons, as opposed to using in-flight decays. To detect the decays of this many stopped muons the detector must subtend a large solid angle and be able to operate at high rates. To distinguish candidate events from the backgrounds requires that the detector elements have high resolutions and an ability to distinguish between charged particles and photons. Finally, to test the apparatus it is useful to have a reference signal. With these points in mind, I will now discuss the observable for the three decay modes and the sources of background signals, then turn to a description of the Crystal Box.

The kinematic observables for the two- and three-body decays are illustrated in fig. 6. They are based on the conservation of energy and momentum in the muon rest frame. The background signals consist of electrons from conventional muon decay ($\mu \rightarrow e \nu \bar{\nu}$) and photons from bremsstrahlung and pair annihilation. The backgrounds divide themselves into two classes: accidental events that superimpose to meet the trigger requirements and prompt events that come from the inner bremsstrahlung process $\mu \rightarrow e \gamma \nu \bar{\nu}$ (fig. 7). The inner bremsstrahlung events also provide the test signal mentioned above.

The Crystal Box is a detector designed to look simultaneously for the three rare muon decays. It consists of a cylindrical drift chamber, a plastic scintillator hodoscope, and a segmented sodium iodide calorimeter. A cutaway diagram of the detector is shown in fig. 8 and a summary of its parameters is shown in fig. 9. A 27 MeV/c μ^+ beam was stopped in a 6.7 cm diameter and 0.57 gm/cm² thick polystyrene target located inside of the drift chamber. The detector elements surround the target and are aligned symmetrically about the beam axis. During the experiment the instantaneous stopping rate varied from 4×10^6 to 8×10^6 muon stops per second. This allowed us to measure the detector's sensitivity to signal pileup and to optimize the stopping rate.

The drift chamber provided position and target vertex location information for charged particles. It consisted of 728 cells arranged in 8 concentric layers. Alternate layers were inclined 12° to 16° from the axis to provide stereo information. The drift chamber hits were recorded by a LRS 4290 TDC system and used in the off-line analysis. The drift chamber was not used in the on-line trigger. The drift chamber was enclosed by the scintillation counter hodoscope.

The plastic scintillation hodoscope consisted of 36 counters viewed on either end by photomultipliers. Each counter shadowed the adjacent row of sodium iodide crystals from the target. In this way the scintillators provided a photon veto signal when used in conjunction with the sodium iodide crystals. The scintillator signals were used to provide the charged particle timing.

The sodium iodide crystals surrounded the rectangular box-shaped enclosure formed by the scintillator hodoscope. Each crystal was 63.5 mm x 63.5 mm square and 304.8 mm long (12 radiation lengths). They were packaged in arrays of 9 crystals across and 10 crystals deep. The individual crystals were optically isolated from each other by white opaque paper (to keep the amount of inactive material in the calorimeter to a minimum). There were four additional arrays of crystals located along the corner intersections of the four quadrants. The entire assembly was sealed in an airtight aluminum container to protect the hygroscopic sodium iodide. The array operated as a shower calorimeter; there was no magnetic field. An energy resolution of 6.3% at 130 MeV was achieved by summing the central 25 crystals around an event. The segmentation of the crystals provided position information for photons and charged particles.

A Monte Carlo simulation was developed to model the detector's operation and to produce the probability distributions used in the analysis (fig. 10). The simulation modeled all the detector elements and the geometry of the Crystal Box. Events were "thrown" from a target according to the measured beam distribution and electrons and photons were transported through the drift chamber to the scintillators. Drift chamber hits were recorded for charged particles. For a target the code used either the polystyrene stopping target, a scintillation counter (called the "I-counter" and used for a timing reference), or a liquid hydrogen target (used in conjunction with a π^- beam for calibration purposes). The code EGS III was then used to model the shower and to estimate the energy deposited in the scintillators and the sodium iodide. The simulated event, which consisted of drift chamber hits and ADC and TDC information, was checked against the trigger logic requirements. If it met the conditions for a trigger then the event was written on an output file in the same format as the real data. All subsequent analysis was done with the off-line replay code. The Monte Carlo generated events and the real data were treated identically.

The energy and timing calibrations of the detectors in the Crystal

Box were carried out with sources and μ^+ and π^- beams on special targets. The techniques used to calibrate the sodium iodide shower calorimeter are shown in fig. 11. The timing calibration techniques are illustrated in fig. 12. These are described below.

The energy calibration of the detector was carried out by several processes and at several energies. A Pu-Be radioactive source that produced a 4.4 MeV photon was used to set the hardware gains. A xenon flash lamp and a system of fiber-optic cables, which coupled the light pulse from the flash lamp to each sodium iodide photomultiplier tube, were used to monitor the stability of the hardware. The energy spectrum of positrons from conventional muon decay was used to provide a midrange energy calibration (i.e., 53 MeV). The measured spectrum and the Monte Carlo simulated spectrum from conventional muon decay are shown in figs. 13 and 14. Several times during the experiment the drift chamber was removed and a liquid hydrogen target was installed inside of the box. The beam line was retuned to transport π^- , which stopped in the hydrogen. The $\pi^- p \rightarrow n \gamma$ reaction produced a 129.4 MeV monoenergetic photon. The measured spectrum is shown in fig. 15. The $\pi^- p \rightarrow n \pi^0$ reaction and the subsequent decay of the π^0 provided photons with energies ranging from 55 MeV to 83 MeV. The two photons from the π^0 decay were also coincident in time and were used to measure the timing resolution of the sodium iodide.

The time delays in the sodium iodide and the plastic scintillation counters were measured with a reference scintillation counter called the "I-counter". The I-counter was located behind a small hole in the polystyrene target and intercepted a small fraction of the muon beam. The muons that stopped in the I-counter and decayed produced positrons that generated signals in the I-counter, the hodoscope, and the sodium iodide at well-defined times. The entire set of 504 detector elements were time-delay compensated with this counter to within one nanosecond of each other.

A time-coincident source of positrons and photons was provided by the inner bremsstrahlung decay $\mu \rightarrow e \gamma \nu \bar{\nu}$. A "time spectrum" for positron-photon ($e \gamma$) coincidences is shown in fig. 16. A "prompt peak" is clearly visible above the random background. (The background part of the spectrum was folded with the detector's time resolution. This is why the background does not appear as flat in the figure.) The background composition may be examined by imposing a kinematic cut on the data. The quantity

$E_e + E_\gamma + |P_e + P_\gamma|$ must be less than or equal to the muon mass for the event to have come from a $\mu \rightarrow e \bar{\nu}_e \nu_\mu$ decay. Events with this quantity being greater than the muon mass could not have come from a $\mu \rightarrow e \bar{\nu}_e \nu_\mu$ decay and represent random background (fig. 17). The $e \bar{\nu}_e \nu_\mu$ time spectrum with this cut imposed is shown in fig. 18. The uncut $e \bar{\nu}_e \nu_\mu$ time spectrum (fig. 16) illustrates the character of the signal $\mu \rightarrow e \bar{\nu}_e \nu_\mu$ decay. The task of extracting the real rare-decay signal from this data is what I would like to discuss next.

The analysis variables for the decay $\mu \rightarrow e \bar{\nu}_e \nu_\mu$ are: the positron energy E_e and the photon energy E_γ (both nominally 52.8 MeV), the angle Θ between them (nominally 180°), and their relative times of detection Δt (they should be coincident, i.e. $\Delta t = 0$). The backgrounds come from the inner bremsstrahlung events $e \bar{\nu}_e \nu_\mu$ and randoms. The analysis variables are summarized in fig. 19. To extract a confidence level for a limit on the branching ratio a maximum likelihood analysis was used. As illustrated in fig. 20, the three processes $e \bar{\nu}_e \nu_\mu$, $e \bar{\nu}_e \nu_\mu$, and randoms contribute to the measured spectrum and have probability densities denoted by P, Q, and R, respectively, that are functions of the analysis variables. Given a sample of N events a likelihood function is constructed and maximized to find the most likely number of $e \bar{\nu}_e \nu_\mu$ and $e \bar{\nu}_e \nu_\mu$ events in the sample. The $e \bar{\nu}_e \nu_\mu$ and the $e \bar{\nu}_e \nu_\mu$ probability densities (P and Q) are estimated from Monte Carlo generated distributions and these are shown in figs. 21 and 22. The randoms distributions are measured by using an out-of-time trigger, and the R probability density is the product of the four distributions (fig. 23).

The value of the likelihood function as a function of the number of $e \bar{\nu}_e \nu_\mu$ and $e \bar{\nu}_e \nu_\mu$ events is shown in fig. 24. The projections onto the $e \bar{\nu}_e \nu_\mu$ and the $e \bar{\nu}_e \nu_\mu$ axes are shown in figs. 25 and 26. For this set 0.97×10^{11} muons were stopped. The sample was restricted to those events with $E_\gamma > 41$ MeV, $E_e > 40.5$ MeV, and $\Theta > 160^\circ$ and contained 1030 events. The maximum likelihood estimate for the number of $e \bar{\nu}_e \nu_\mu$ events in this sample is 215 ± 20 . The Monte Carlo simulation predicts 245 events. The probability of a $\mu \rightarrow e \bar{\nu}_e \nu_\mu$ event with E_γ and E_e near 52.8 MeV falls from 10^{-6} at 36 MeV to 10^{-9} at 47 MeV, as shown in fig. 27, and provides a rather critical test of the detector's operation. The agreement between the observed and the predicted number of $e \bar{\nu}_e \nu_\mu$ events gives us confidence that the calibrations and resolutions of the detector and the normalization are understood. The maximum likelihood estimate for the number of $e \bar{\nu}_e \nu_\mu$ events has a maximum at zero events and has less than 3 events at the 90% confidence level. The

product of the acceptance and the efficiency is 22%. With these values the limit on the branching ratio for the decay $\mu \rightarrow e \gamma \gamma$ is then less than 1.4×10^{-10} . These results are summarized in fig. 28.

The analysis of the $\mu \rightarrow e \gamma \gamma$ events is in the preliminary stage. We are working to understand the nature of the backgrounds. At this time we do not feel confident enough to employ a likelihood analysis; instead we have used a correlated-cut probability analysis. The analysis variables for this three-body decay are the total energy, a time coincidence, and the sum of the vector momentum. The background events arise from three-fold accidental coincidences, $e \gamma \gamma$ events in time with a random photon, and two-fold photons in time with a random electron. These are illustrated in fig. 29. To carry out the cut analysis the probability that each event in the sample was consistent with the kinematics of a decay into three bodies was computed (fig. 30). The probability densities for each of the analysis variables were derived from the Monte Carlo simulation. A data event was assigned a probability in each of the four variables and their product was calculated. The resulting number of events with a given probability density was then plotted in a histogram. For comparison purposes a Monte Carlo simulation of the muon-number-violating decay $\mu \rightarrow e \gamma \gamma$, based on a general local interaction, was used to produce an analogous histogram. These histograms are shown in fig. 31. (In these figures the negative of the logarithm of the probability density is plotted, so increasing probability density is to the left.) In a sample containing 2.2×10^{11} stopped muons, with a final acceptance and efficiency product of 3.05%, the upper limit for the branching ratio of the decay $\mu \rightarrow e \gamma \gamma$ is less than 3.8×10^{-10} at the 90% confidence level. These results are summarized in fig. 32.

These results are preliminary and are based on a fraction of our total data. The results for the data analyzed to date are summarized in fig. 33. A total of 9.5×10^{11} muons were stopped in the experiment. The analysis of the remaining data is underway and we expect to achieve final sensitivities of a few times 10^{-11} . At this time we see no evidence for the nonconservation of separate family numbers in muon decay.

Figure Captions

Fig. 1	The Crystal Box collaboration
Fig. 2	Comments on the Standard Model
Fig. 3	Rare muon-decay experiment history
Fig. 4	Published limits prior to this experiment
Fig. 5	Experiment design
Fig. 6	Kinematics and observables
Fig. 7	Backgrounds
Fig. 8	Cutaway drawing of the Crystal Box
Fig. 9	Parameters of the Crystal Box
Fig. 10	Monte Carlo simulation
Fig. 11	Calibration of the sodium iodide for energy
Fig. 12	Calibration of the Crystal Box for timing
Fig. 13	Detected Michel positron spectrum
Fig. 14	Monte Carlo predicted Michel positron spectrum
Fig. 15	Detected photon energy for $\pi^- p \rightarrow n \gamma$
Fig. 16	e^+e^- timing spectrum
Fig. 17	Single muon decay kinematic cut parameter
Fig. 18	e^+e^- random background
Fig. 19	$\mu^+ \rightarrow e^+ \gamma$ analysis variables and backgrounds
Fig. 20	Maximum likelihood analysis
Fig. 21	Monte Carlo generated e^+e^- probability distributions
Fig. 22	Monte Carlo generated $e^+e^- \gamma$ probability distributions
Fig. 23	Random background measured distributions
Fig. 24	$e^+e^- \rightarrow e^+e^- \gamma$ likelihood plot
Fig. 25	$e^+e^- \gamma$ projection of likelihood plot
Fig. 26	e^+e^- projection of likelihood plot
Fig. 27	Probability for $\mu \rightarrow e^+e^- \gamma$ with energies $> \text{ENERGY}$
Fig. 28	e^+e^- summary
Fig. 29	$\mu \rightarrow e^+e^- \gamma$ analysis variables and backgrounds
Fig. 30	$\mu \rightarrow e^+e^- \gamma$ probability analysis
Fig. 31	Correlated cut analysis histograms
Fig. 32	$e^+e^- \gamma$ summary
Fig. 33	Branching-ratio upper-limit summary

RARE MUON DECAYS

THE CRYSTAL BOX COLLABORATION

LOS ALAMOS NATIONAL LABORATORY

**R.D. BOLTON
J.D. BOWMAN
R. CARLINI
M.D. COOPER
M. DUONG-VAN
J.S. FRANK
A.L. HALLIN
P. HEUST
C.M. HOFFMAN
G.E. HOGAN**

**P.O. MARIAM
H.S. MATIS
R.E. MISCHKE
D.E. NAOLE
V.D. SANDBERG
G.H. SANDERS
U. SENNHAUSER
R.L. TALAGA
R.W. VERBECK
R.A. WILLIAMS**

UNIVERSITY OF CHICAGO

D.P. GROSNICK

S.C. WRIGHT

HANSEN LABORATORY, STANFORD UNIVERSITY

**S.L. WILSON
L.B. HUGHES**

R. HOPSTADTER

TEMPLE UNIVERSITY

V.L. HIGHLAND

J. McDONOUGH

THE STANDARD MODEL

Conserves Lepton Family Number

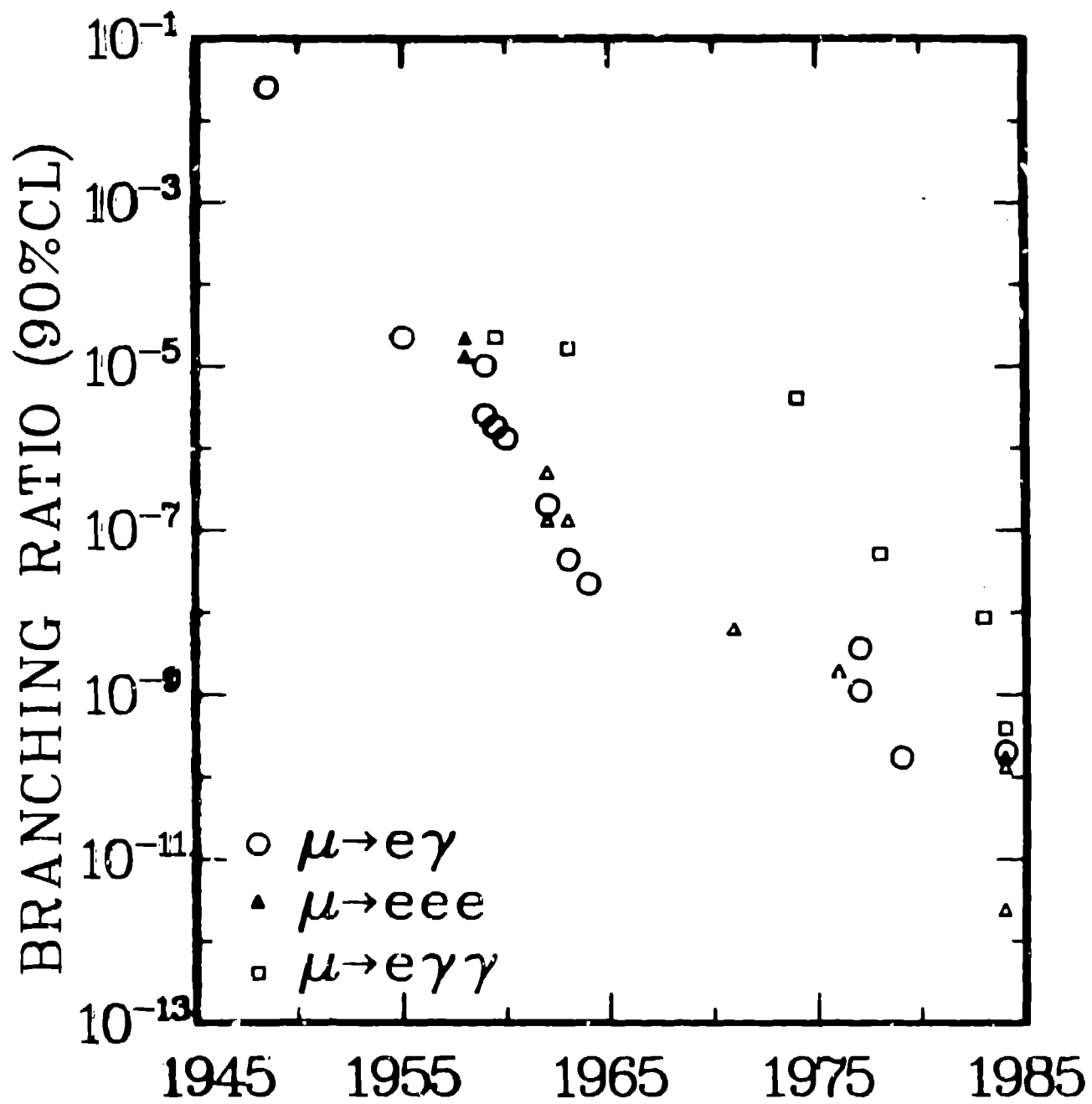
It Is Consistent -- But Incomplete

Tests of Lepton Family Number Conservation

- **Muon Decays**
- **Neutrino Oscillations**

**Extensions of The Standard Model Should
Be Compatible With the Measured Limits
For These Processes**

RARE MUON DECAY EXPERIMENTAL HISTORY



PUBLISHED LIMITS PRIOR TO THIS EXPERIMENT

$$\frac{\Gamma(\mu \rightarrow e \gamma)}{\Gamma(\mu \rightarrow e \nu \bar{\nu})} < 1.7 \times 10^{-10}$$

$$\frac{\Gamma(\mu \rightarrow e \gamma \gamma)}{\Gamma(\mu \rightarrow e \nu \bar{\nu})} < 8.4 \times 10^{-9}$$

$$\frac{\Gamma(\mu \rightarrow e e e)}{\Gamma(\mu \rightarrow e \nu \bar{\nu})} < 2.4 \times 10^{-12}$$

EXPERIMENT DESIGN

To ~~measure~~ a branching ratio of 10^{-10} requires
a ~~sample~~ containing 10^{11} events.

Solid angle

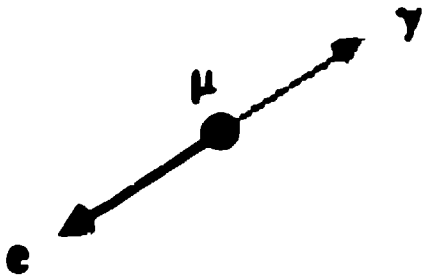
Rate

Resolution to distinguish background

A reference signal to test the apparatus

KINEMATICS, OBSERVABLES

$$\underline{\mu \rightarrow e \gamma}$$



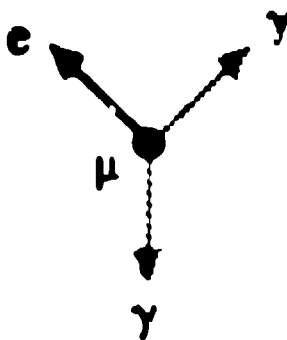
$$E_e = \frac{m_\mu}{2} = 52.8 \text{ MeV}$$

$$E_\gamma = \frac{m_\mu}{2} = 52.8 \text{ MeV}$$

$$\theta = 180^\circ$$

$$\Delta t = 0$$

$$\underline{\mu \rightarrow e \gamma \gamma}$$

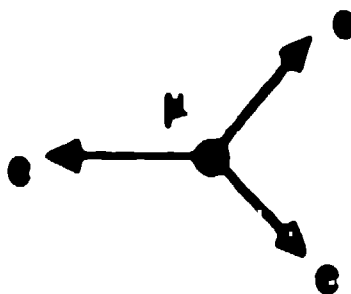


$$E_e + E_{\gamma_1} + E_{\gamma_2} = m_\mu$$

$$\vec{p}_e + \vec{p}_{\gamma_1} + \vec{p}_{\gamma_2} = 0$$

$$\Delta t = 0$$

$$\underline{\mu \rightarrow e e e}$$



$$E_1 + E_2 + E_3 = m_\mu$$

$$\vec{p}_1 + \vec{p}_2 + \vec{p}_3 = 0$$

$$\Delta t = 0$$

Common vertex

BACKGROUNDS

Accidental coincidences:

**e : Michel positrons from normal
muon decay**

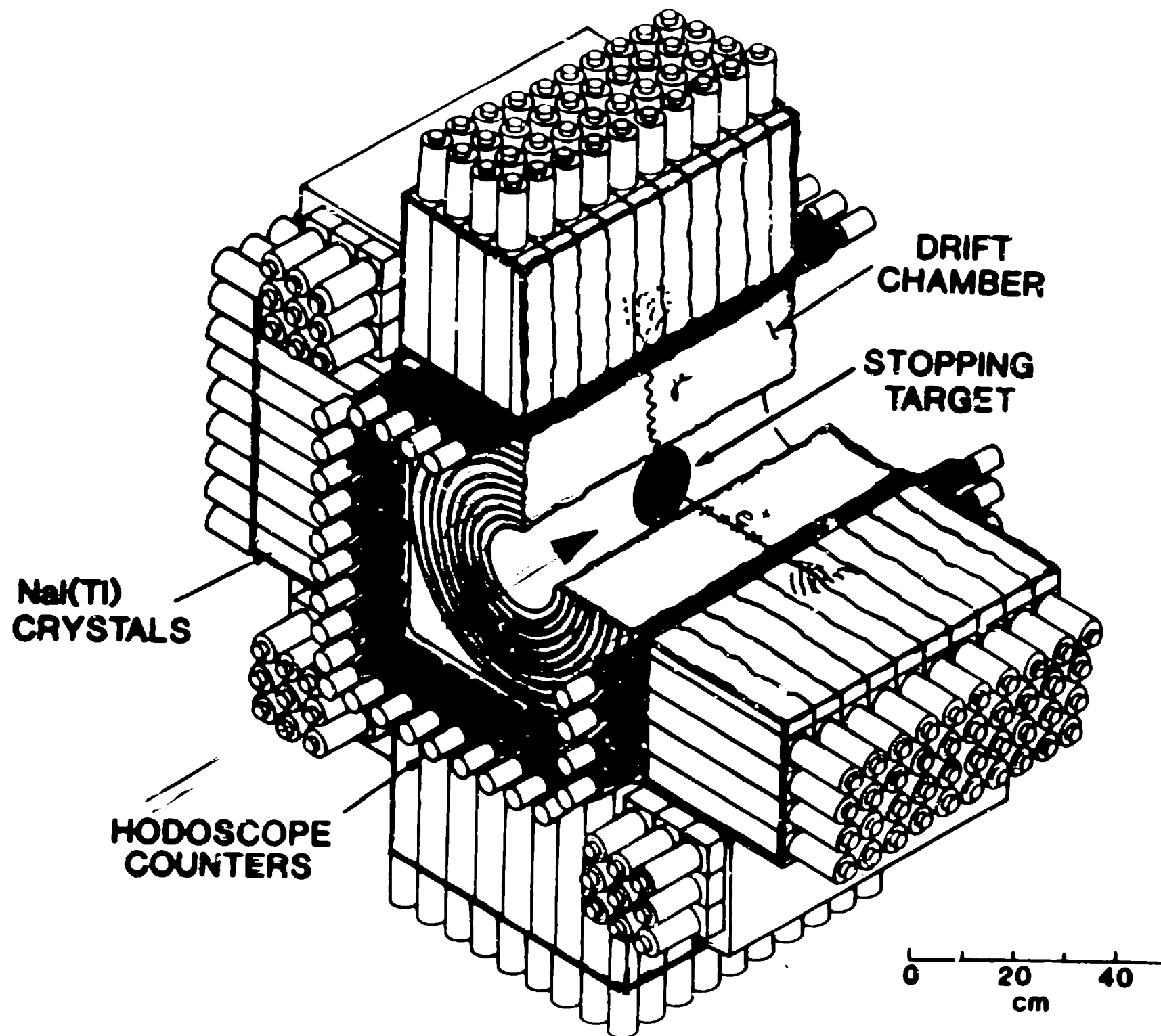
γ : Bremsstrahlung

Positron annihilation

Misidentified electrons

Prompt background:

Inner bremsstrahlung $e \gamma \nu \bar{\nu}$



PARAMETERS OF THE CRYSTAL BOX

Target

polystyrene

radius

6.7 cm

thickness

52 mg/cm

Drift chamber

8 planes

728 sense wires

track efficiency

95%

thickness

6.7×10^{-3} rad length

position res on target

2 mm

Scintillator hodoscope

36 scintillators

1/2 in thick

time resolution

290 ps (FWHM)

NaI

360 face crystals

$6.35 \times 6.35 \times 30.5$ cm

36 corner crystals

resolution timing

12 ns

energy

8% @ 50 MeV

MONTÉ CARLO SIMULATION

Code models detector elements and geometry of the Crystal Box

Events:

- beam distribution**
- "I-counter"**
- liquid hydrogen target**

EGS 3 shower code

Gives simulated events in the same format as the real data

Further analysis uses the same replay code, so data and Monte Carlo events are treated identically

CALIBRATION

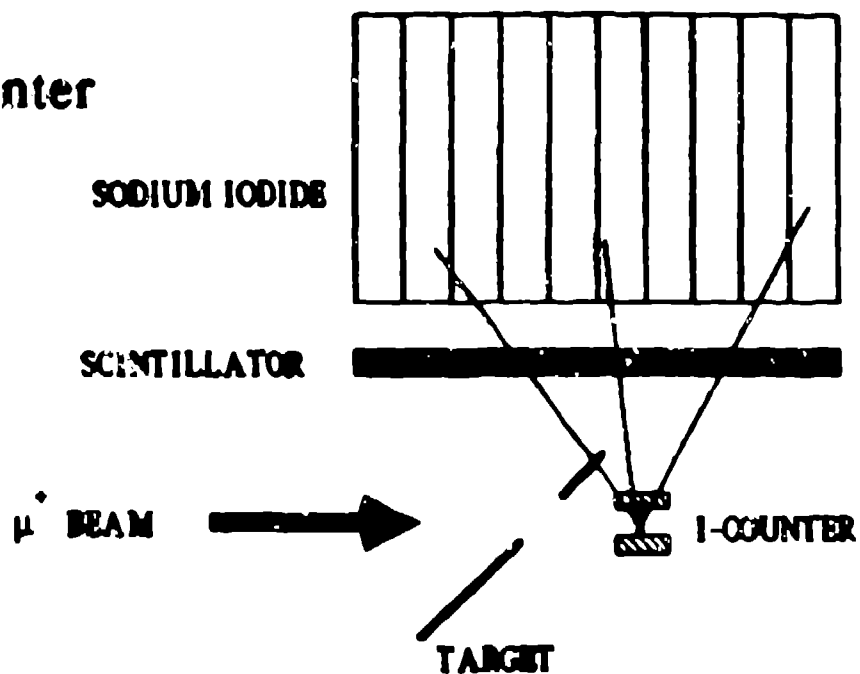
SODIUM IODIDE ENERGY

- Pu-Be SOURCE $E_{\gamma} = 4.4 \text{ MeV}$
- $\pi^{-} p \rightarrow n \gamma$ $E_{\gamma} = 129.4 \text{ MeV}$
- $\pi^{-} p \rightarrow n \pi^{0}$
 $\searrow \gamma\gamma$ $55 \text{ MeV} < E_{\gamma} < 83 \text{ MeV}$
- $\mu \rightarrow e \nu \bar{\nu}$ Positron Energy Spectrum
- Light Flasher - Fiber Optic System

CALIBRATION

TIMING

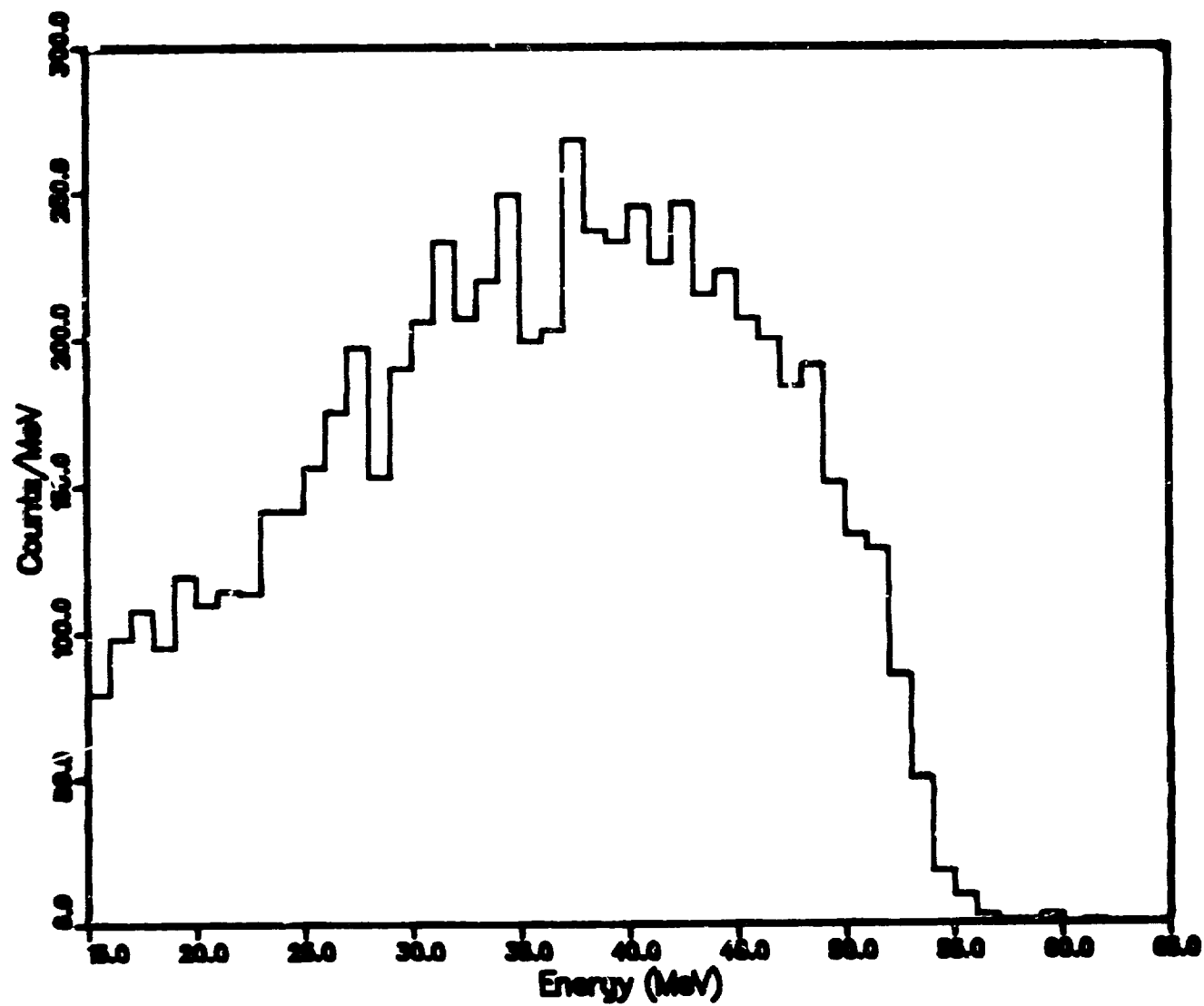
- I-Counter



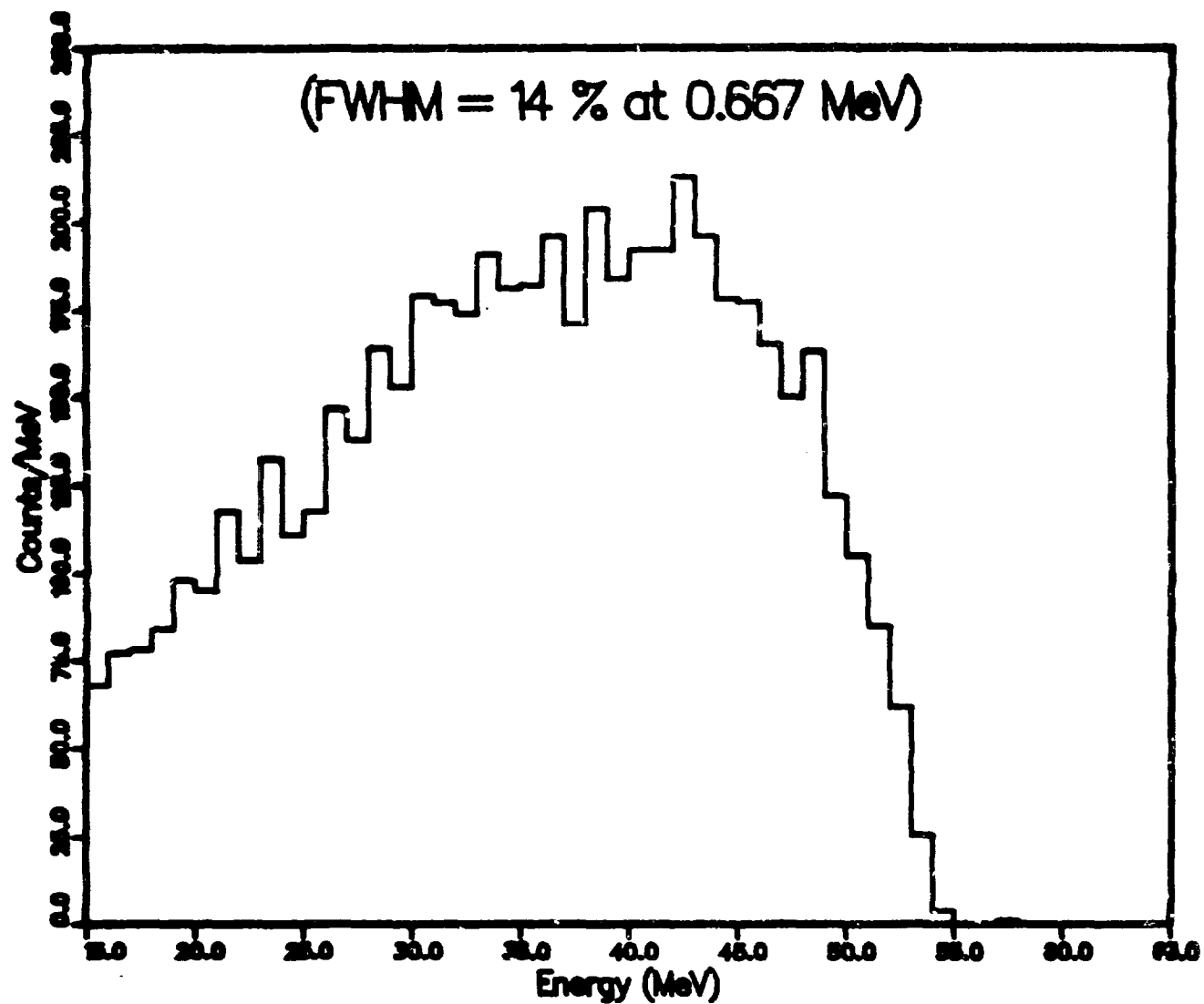
- $\pi^0 \rightarrow \gamma\gamma$

- $\mu \rightarrow e\gamma\nu\bar{\nu}$

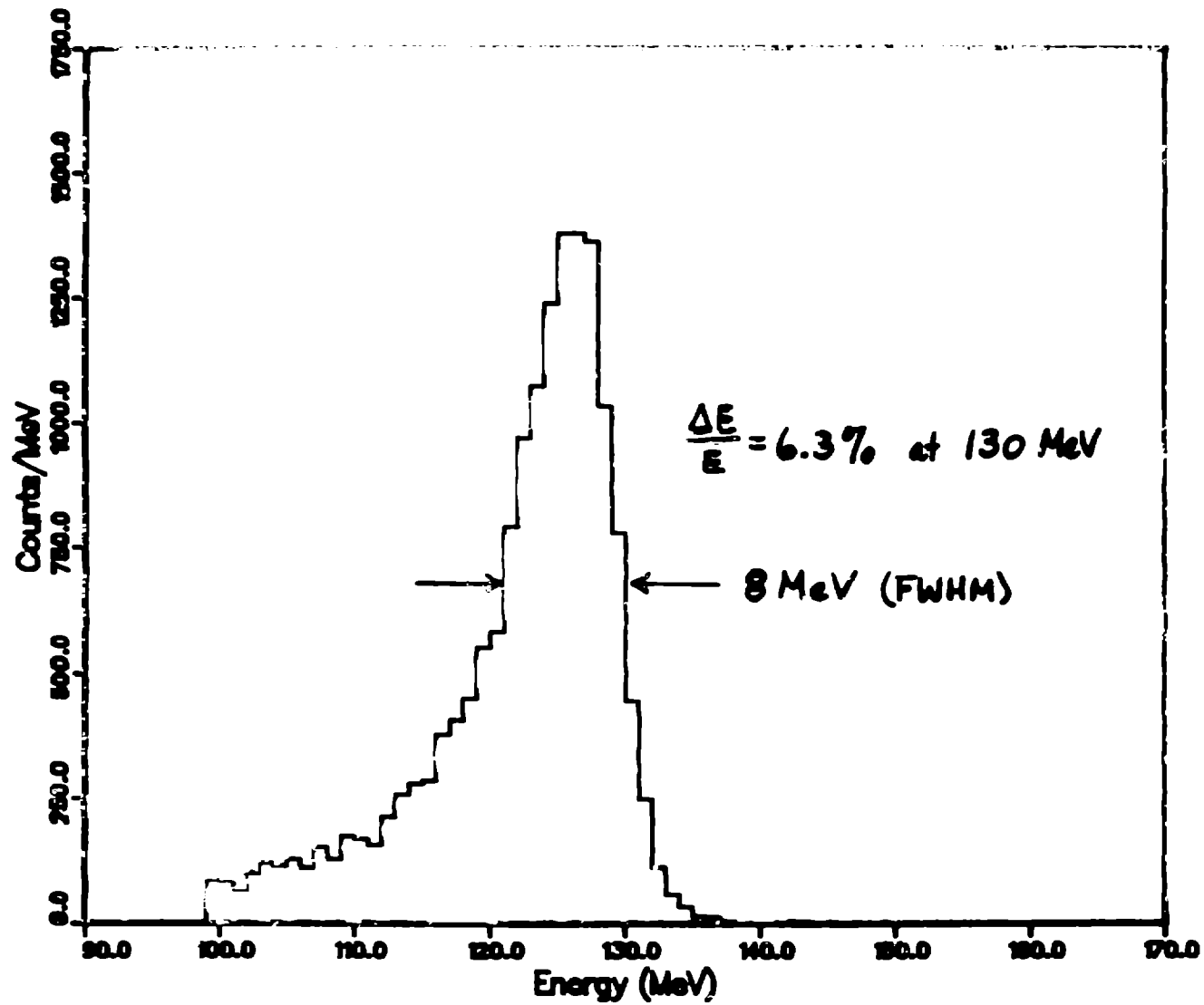
Detected Michel Positron Spectrum



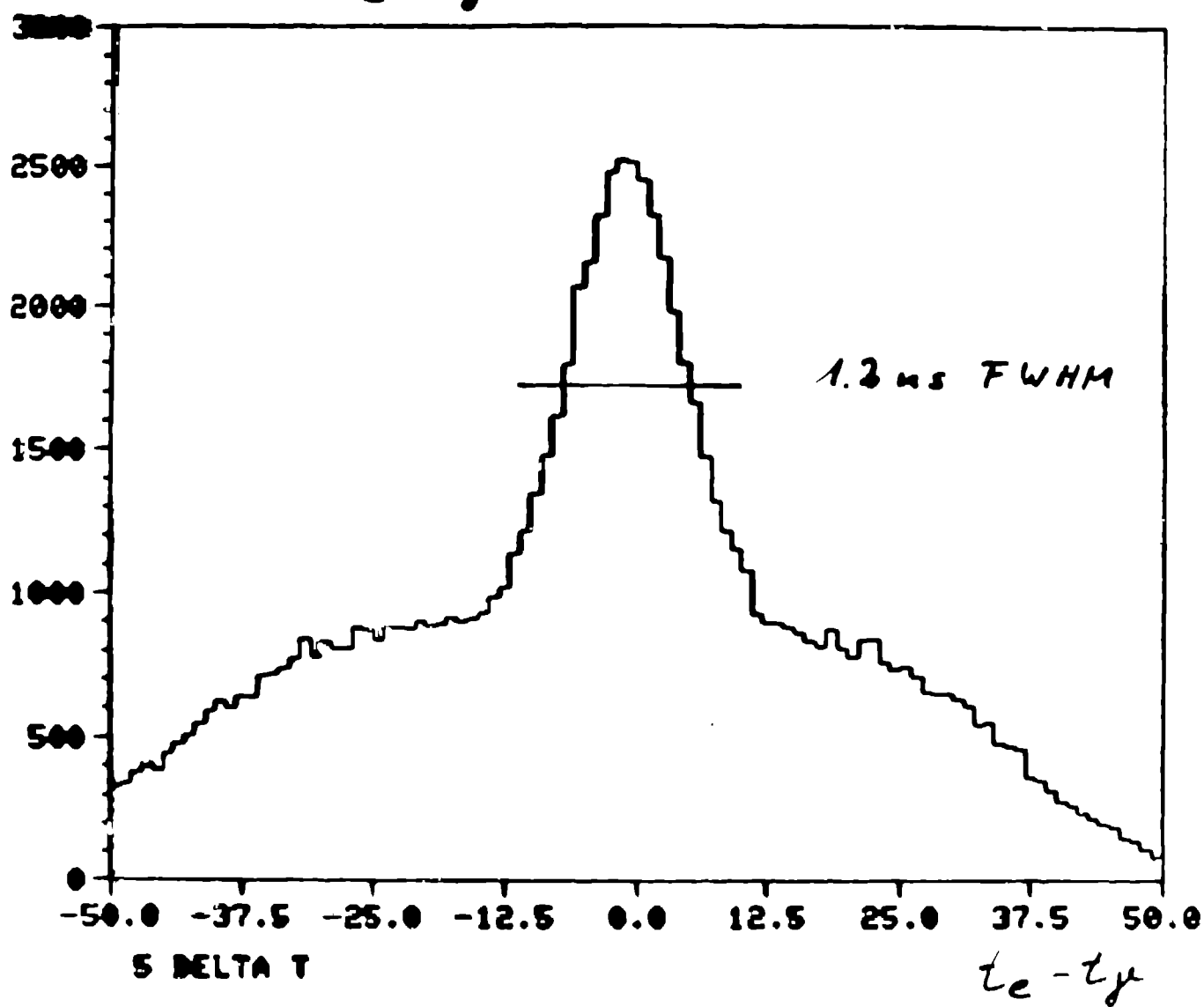
Predicted Michel Positron Spectrum

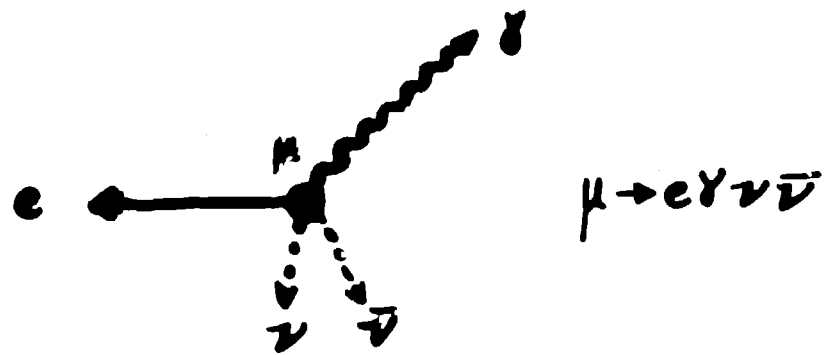


Detected Photon Energy for $\pi^- p \rightarrow n \gamma$



$$E_e + E_\gamma + |\vec{p}_e + \vec{p}_\gamma| < 110 \text{ MeV}$$

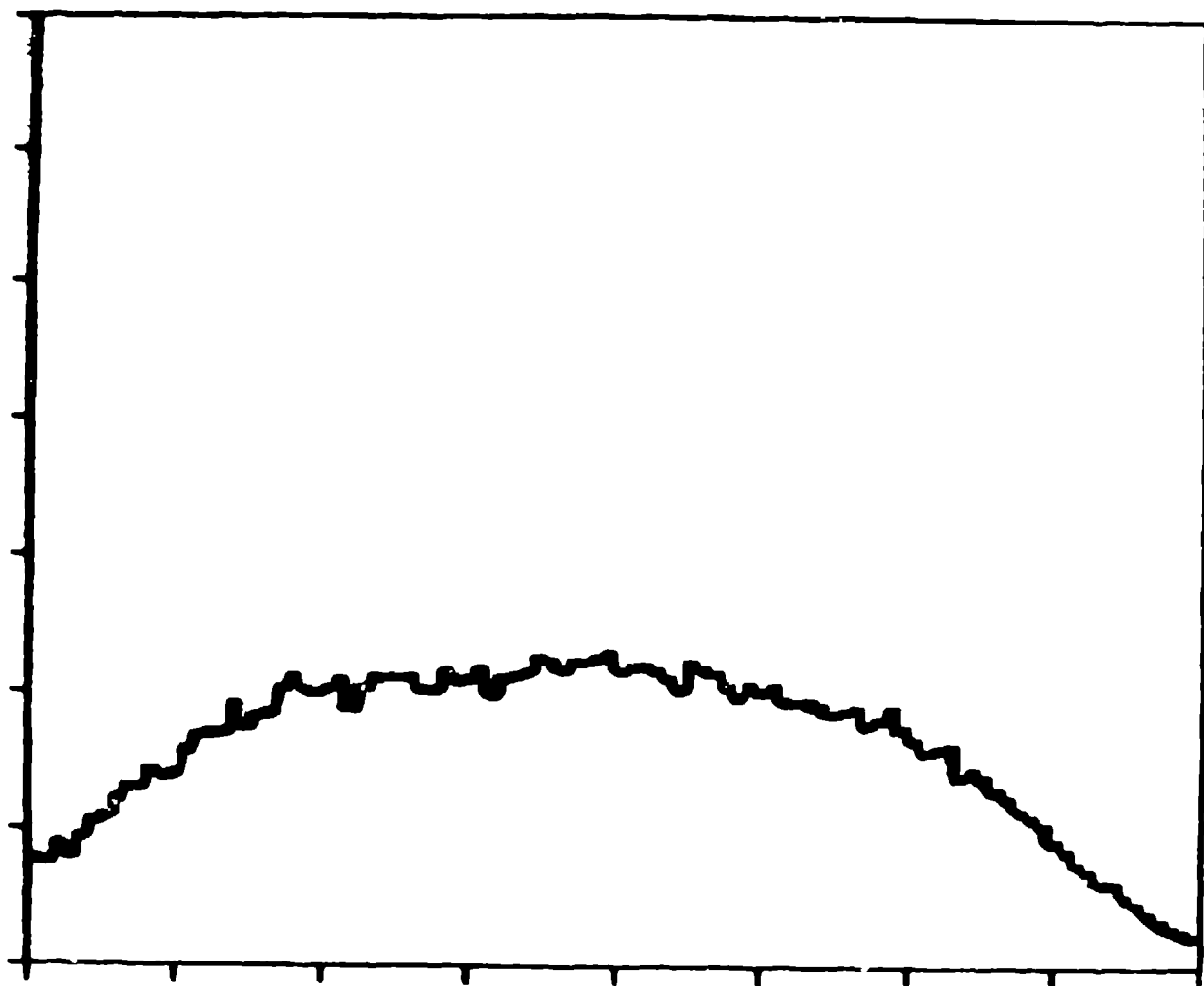




$$E_e + E_\gamma + |\vec{p}_e + \vec{p}_\gamma| \leq m_\mu$$

- Events satisfying this inequality have the possibility of coming from a muon decay with inner bremsstrahlung
- Events $> m_\mu$ must be randoms

$$E_e + E_\gamma + |\vec{p}_e + \vec{p}_\gamma| \geq 115 \text{ MeV}$$



pure random background



Analysis Variables:

- Positron Energy..... 52.8 MeV
- Photon Energy..... 52.8 MeV
- Angle..... 180°
- Timing..... coincident

Backgrounds:

- Inner Bremsstrahlung $e \gamma \nu \bar{\nu}$ prompt
- Randoms

MAXIMUM LIKELIHOOD ANALYSIS

Four independent variables describe the events

$$\vec{x} = (E_e, E_\gamma, \theta, \Delta t)$$

Three processes contribute to the measured spectrum:
($e\gamma$, $e\gamma\nu\bar{\nu}$, random)

$P(\vec{x})$ = probability density for $e\gamma$ at \vec{x}

$Q(\vec{x})$ = probability density for $e\gamma\nu\bar{\nu}$ at \vec{x}

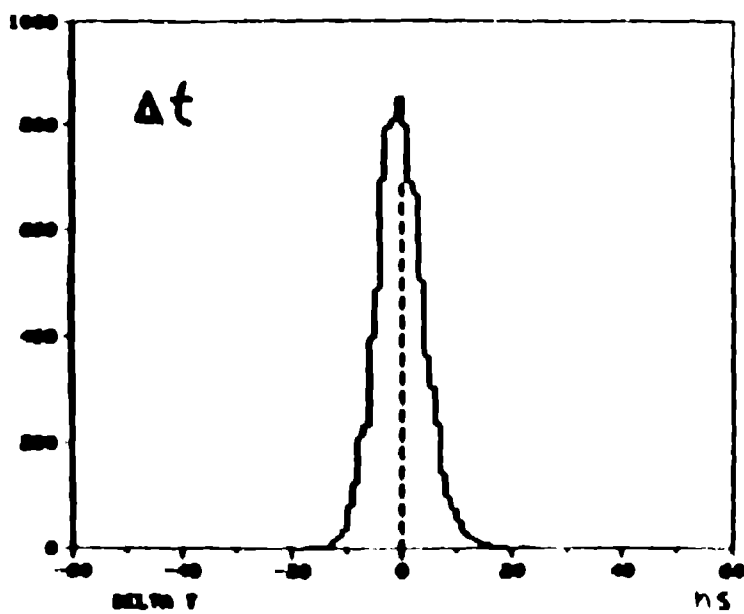
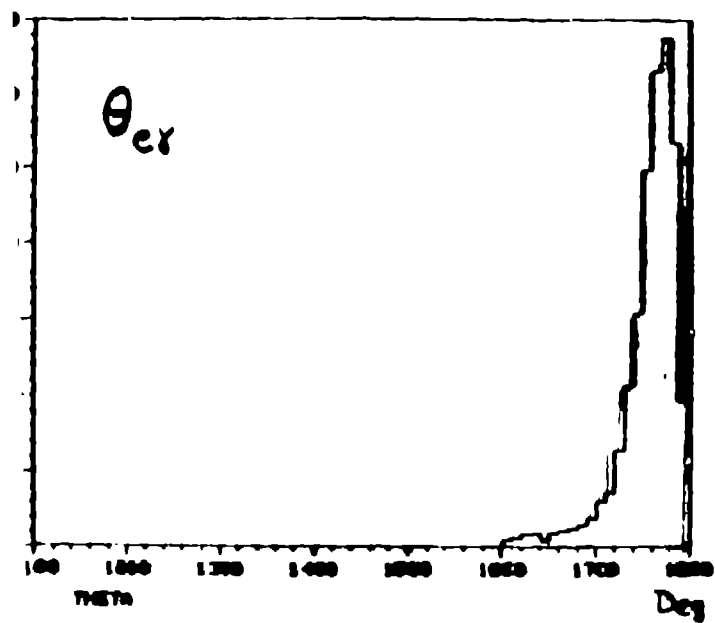
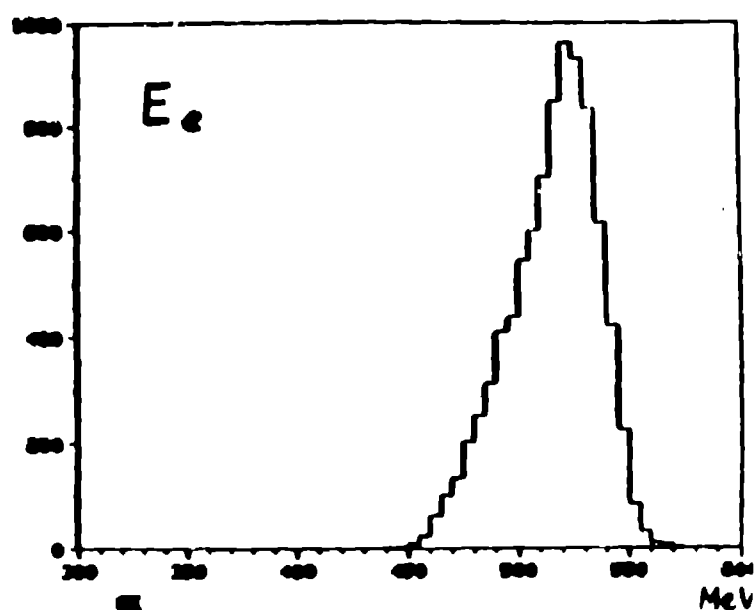
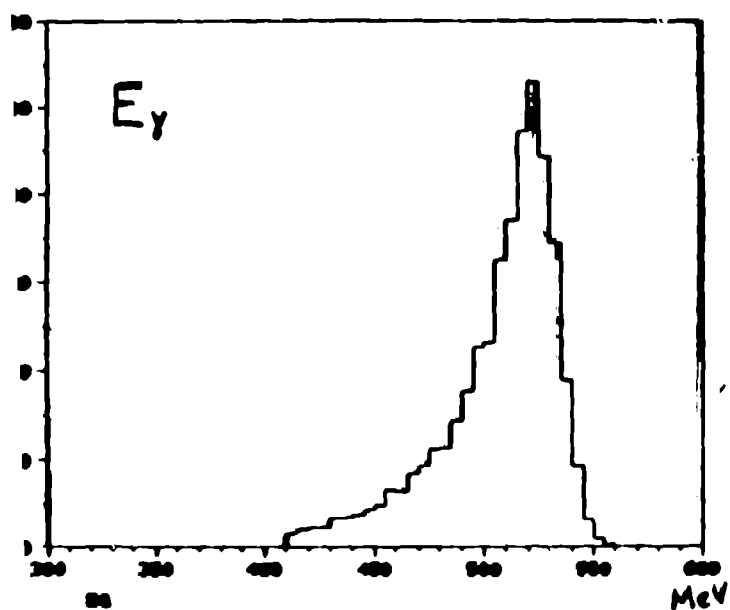
$R(\vec{x})$ = probability density for random at \vec{x}

Given a sample of N events,
solve for α and β to give maximum likelihood

$$\mathcal{L}(\alpha, \beta) = \prod_{i=1}^N \left[\frac{\alpha}{N} P(\vec{x}) + \frac{\beta}{N} Q(\vec{x}) + \frac{(N-\alpha-\beta)}{N} R(\vec{x}) \right]$$

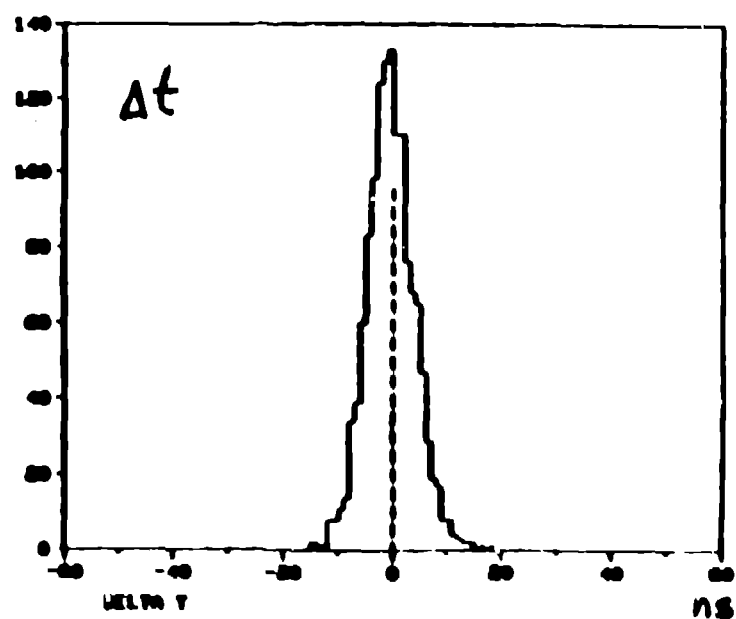
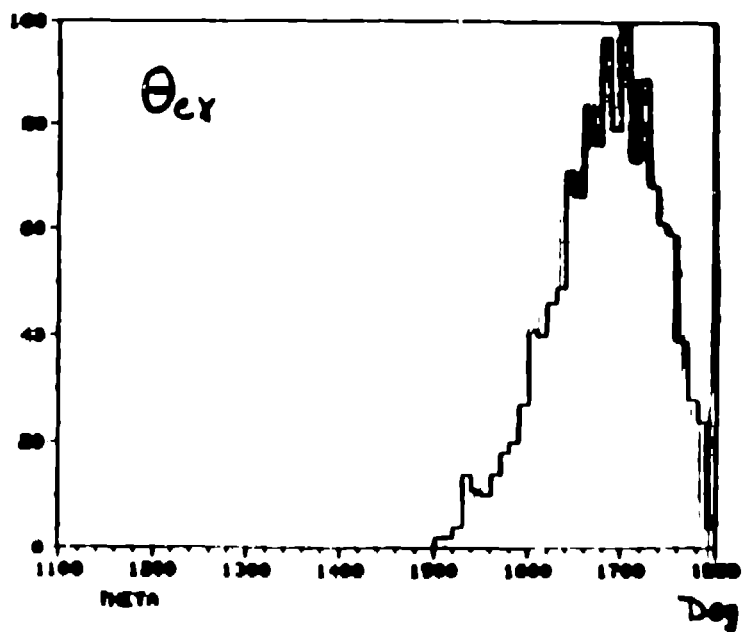
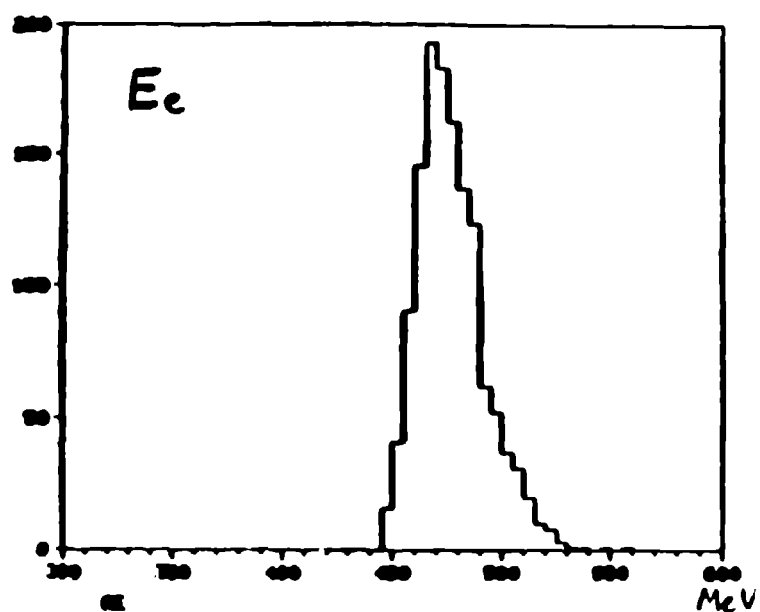
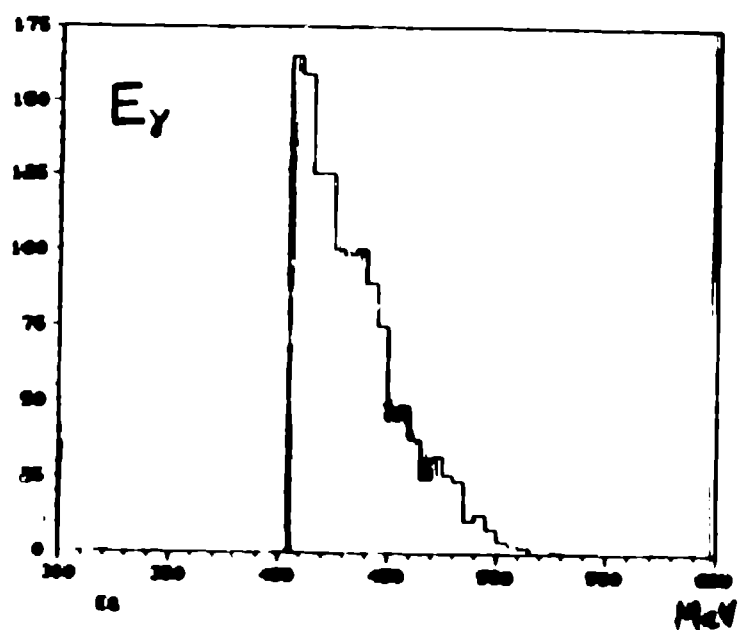
c

MONTÉ CARLO GENERATED $\mu \rightarrow e \gamma$ DISTRIBUTIONS



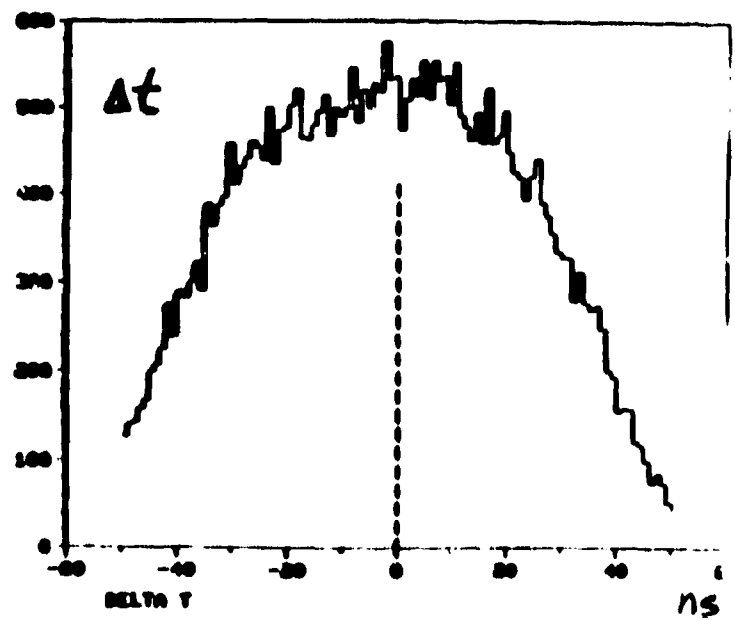
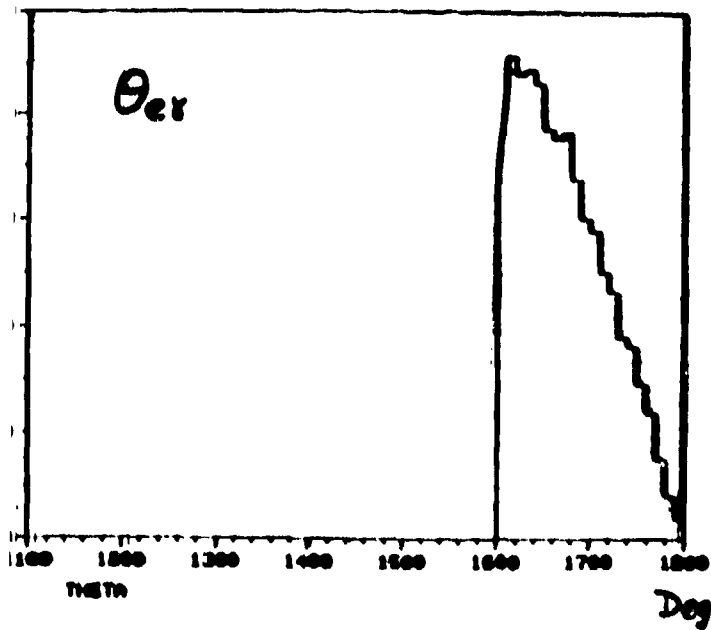
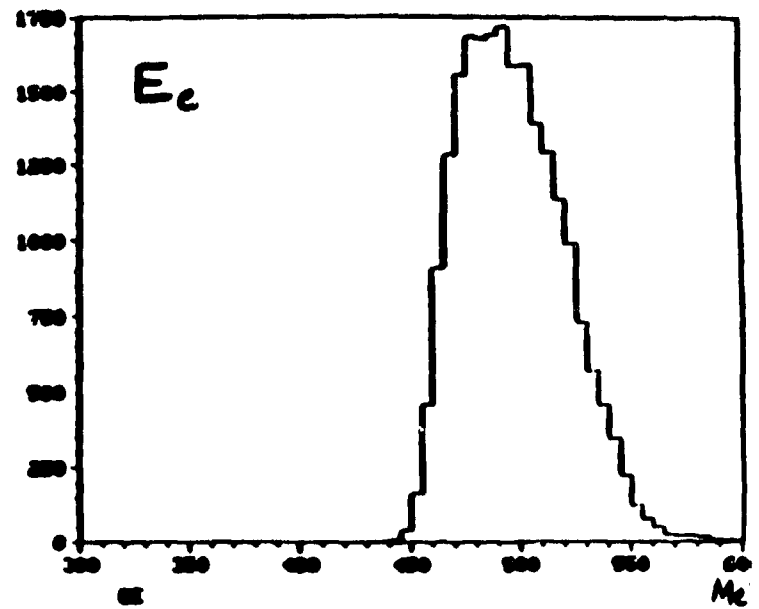
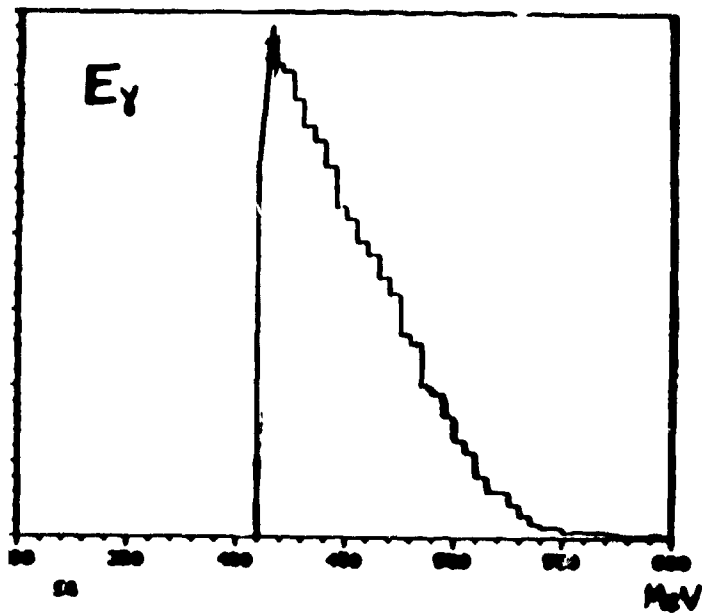
4c

MONTE CARLO GENERATED $\mu \rightarrow e \gamma \nu \bar{\nu}$ DISTRIBUTIONS

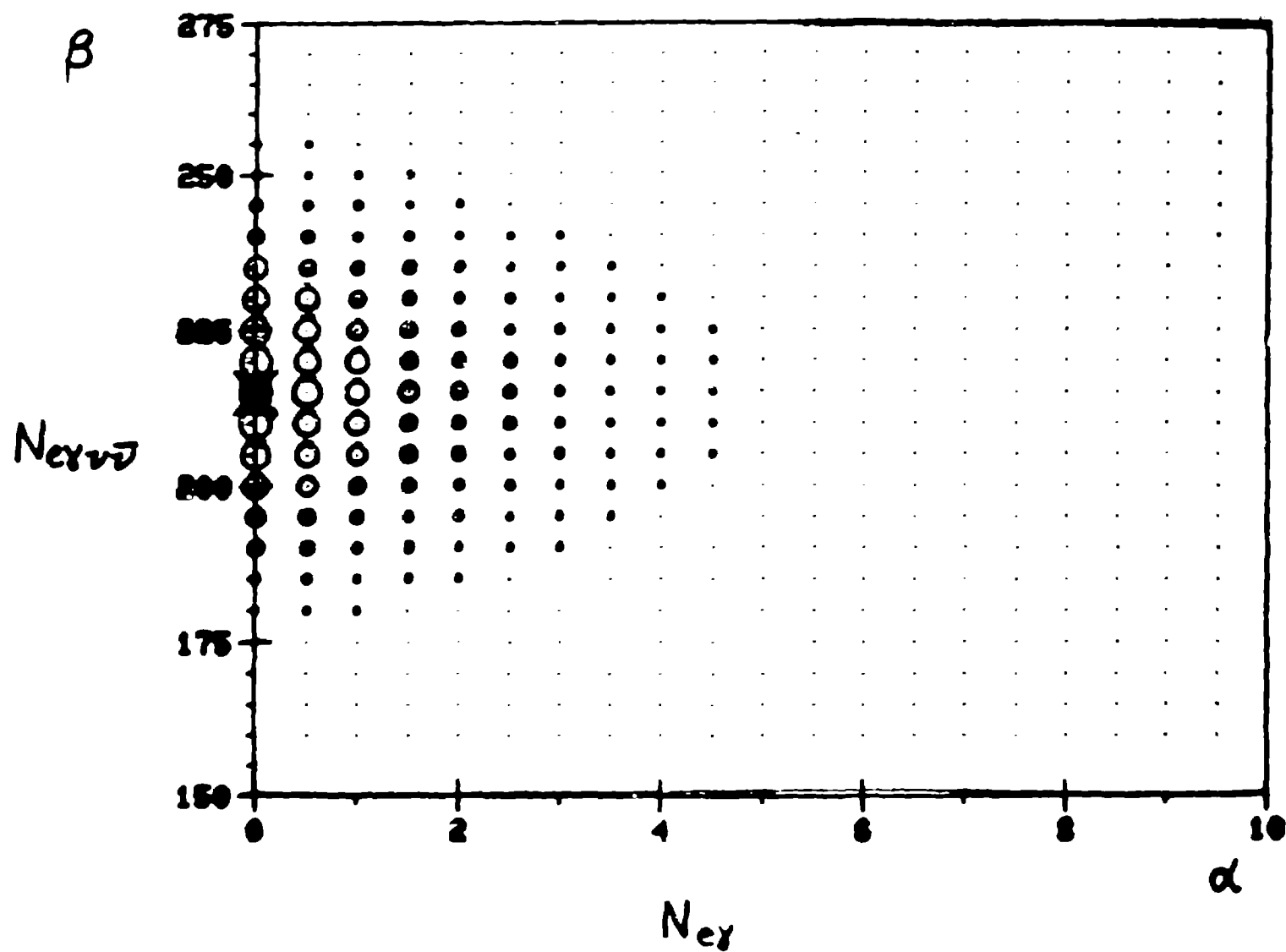


RANDOM BACKGROUND

DISTRIBUTIONS

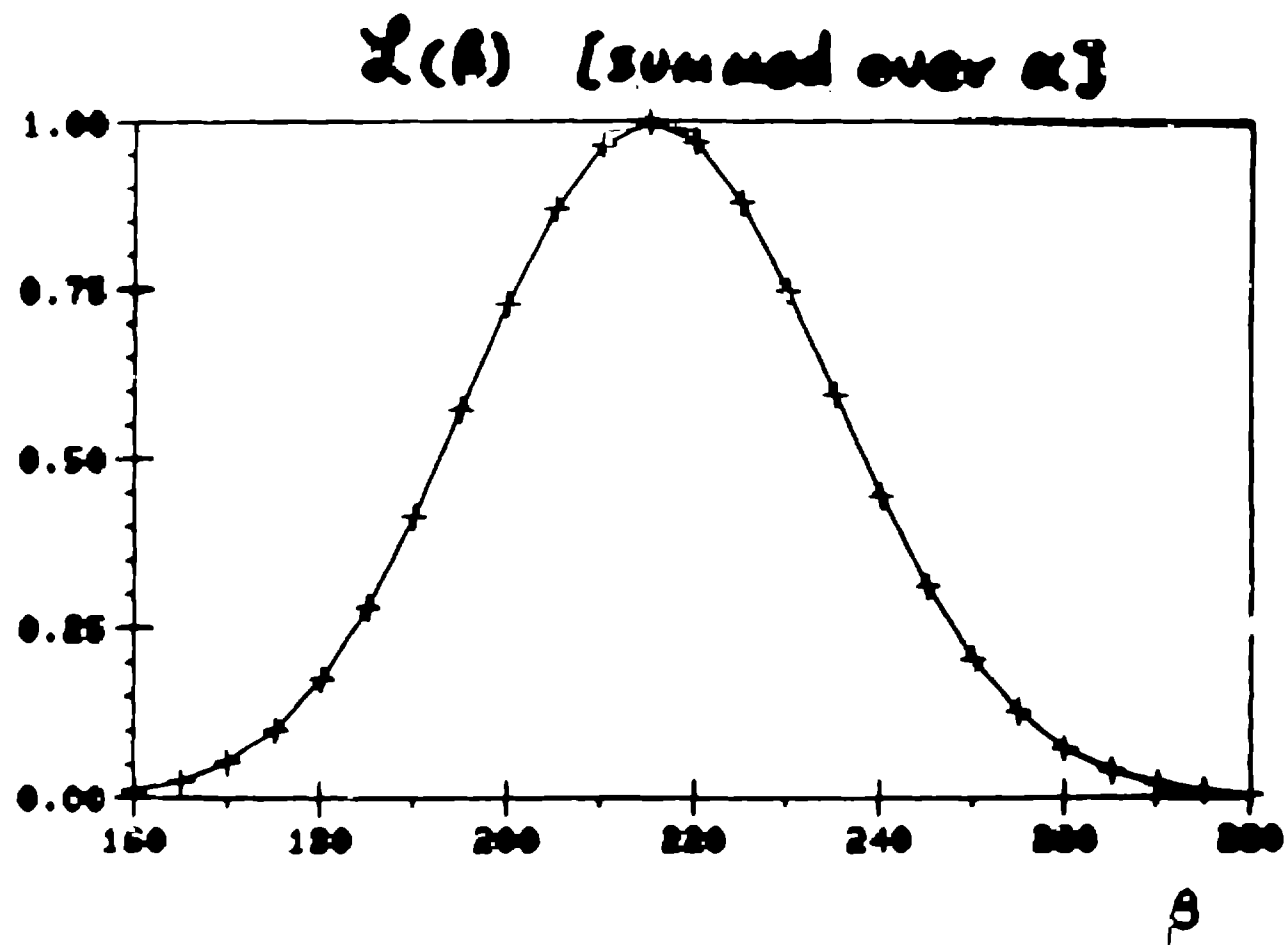


$L(\alpha, \beta)$



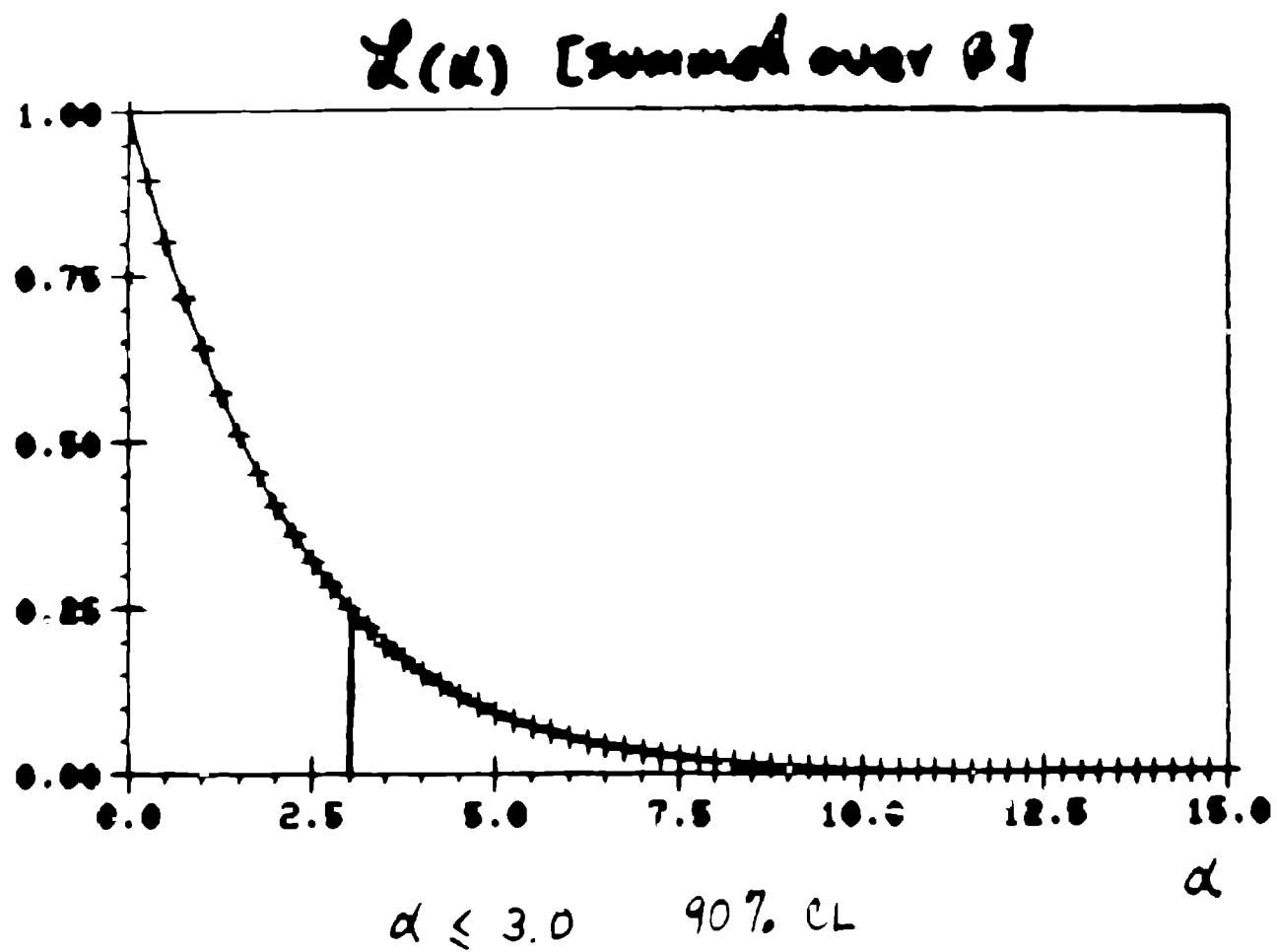
1030 events

$E_x > 41, \quad E_e > 40.5, \quad \theta > 160^\circ$

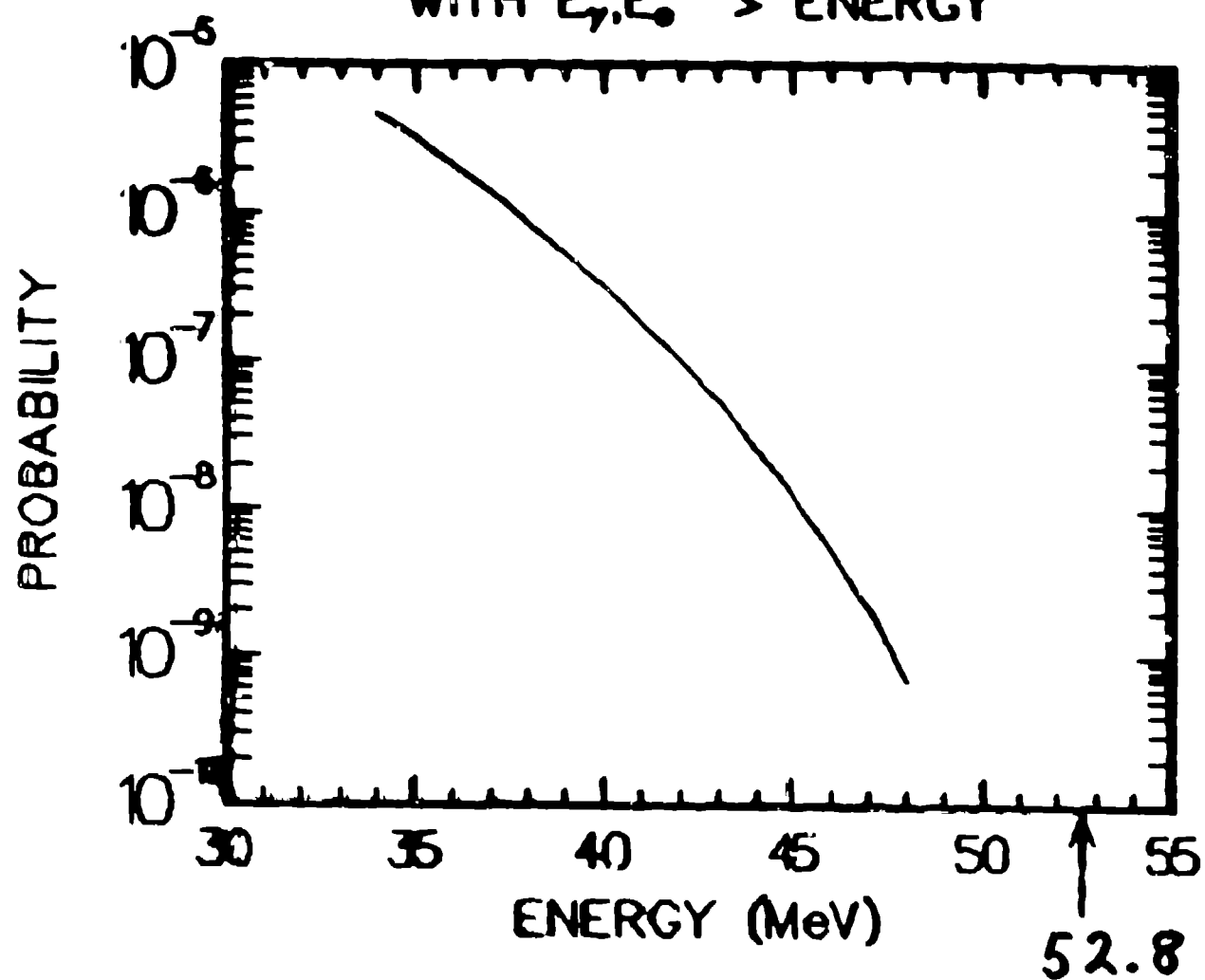


$e\gamma\nu\bar{\nu}$: 215 ± 20

expected: 245



PROBABILITY FOR $\mu \rightarrow e \gamma \nu \bar{\nu}$
WITH $E_\gamma, E_e > \text{ENERGY}$



$e\gamma$ SUMMARY

0.97×10^{11} MUONS STOPPED

$e\gamma\nu\bar{\nu}$ β OBSERVED: 215 ± 20

EXPECTED: 245

$e\gamma$ α MAXIMUM: $\alpha = 0$

90% CL : $\alpha \leq 3.0$

Acceptance x Efficiency - 22 %

Branching Ratio < 1.4×10^{-10}

$$\underline{\mu^+ \longrightarrow e^+ \gamma\gamma}$$

Analysis Variables:

• Total energy 106 MeV

• Timing $\Delta t = 0$

• Vector Momentum in
Decay Plane

• Coplanarity

$$\sum_i \vec{p}_i = 0$$

Backgrounds:

• Triple randoms

• $e \gamma \nu \bar{\nu} : \gamma_{\text{random}}$

• $(\gamma\gamma) : e_{\text{random}}$

$\mu \rightarrow e \gamma \gamma$ PROBABILITY ANALYSIS

Four variables:

$$E_{\text{tot}} = E_e + E_{\gamma_1} + E_{\gamma_2}$$

$$\tau_{\text{rms}} = \sqrt{\Sigma(t - t_i)^2}$$

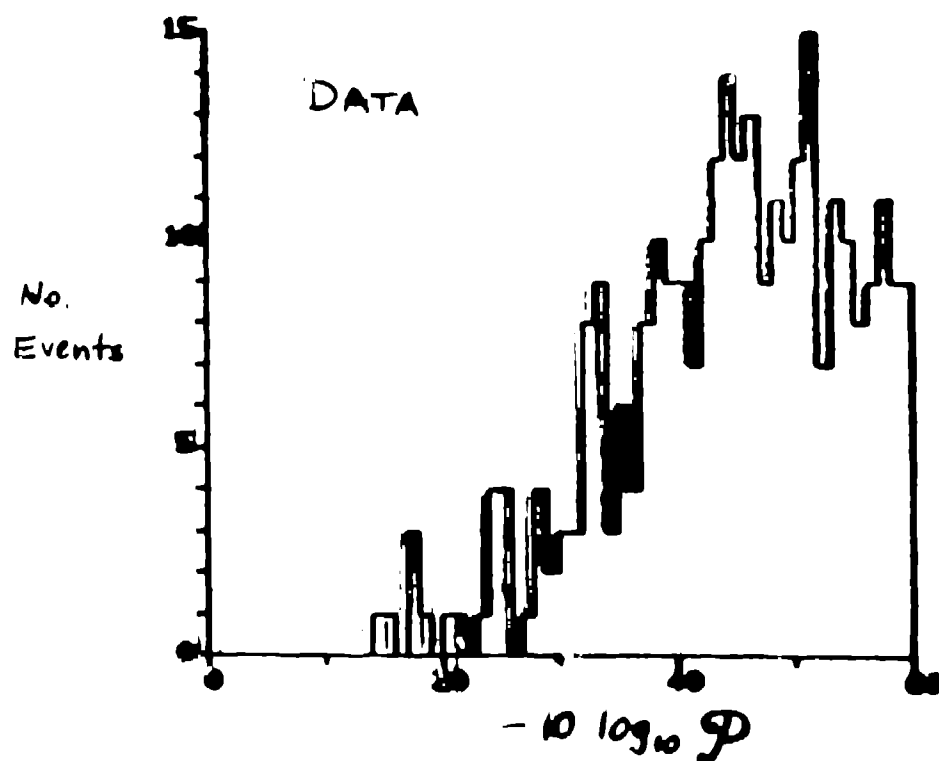
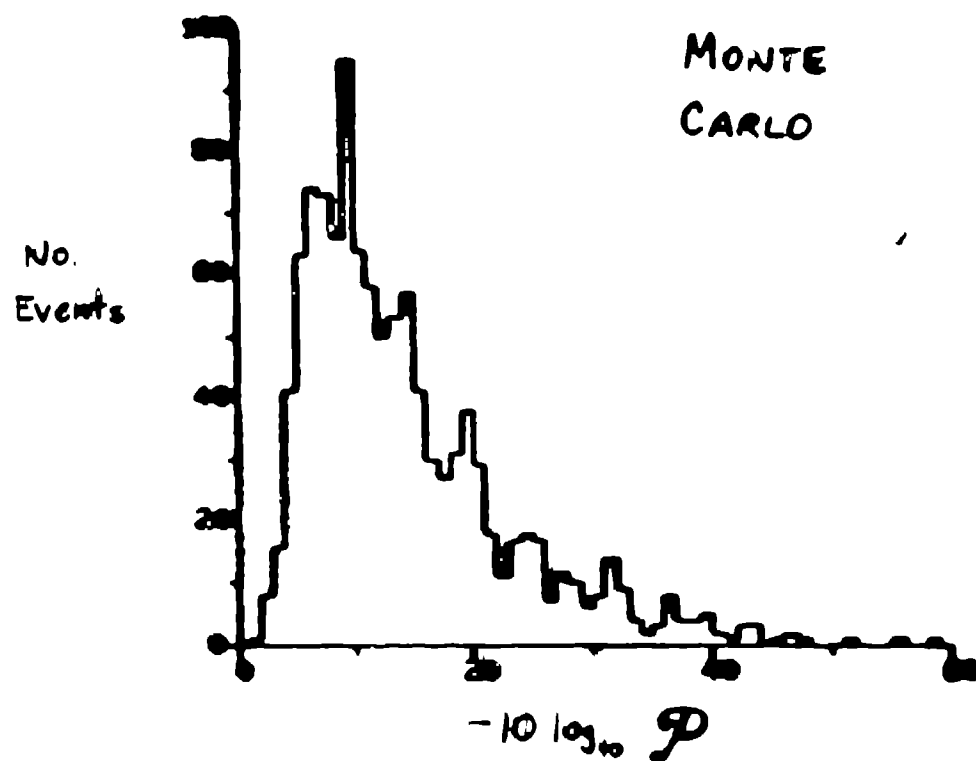
$$|\vec{P}_{\parallel}|$$

$$|\vec{P}_{\perp}|$$

$$|\vec{P}|$$

$$\mathcal{P}(\vec{x}) = p_1(E_{\text{tot}}) \times p_2(\tau_{\text{rms}}) \times p_3(|\vec{P}_{\parallel}|) \times p_4\left(\frac{|\vec{P}_{\perp}|}{|\vec{P}|}\right)$$

CORRELATED CUT ANALYSIS



$e\gamma\gamma$ SUMMARY

2.2×10^{11} MUONS STOPPED

Acceptance x Efficiency = 3.05 %

BRANCHING RATIO < 3.8×10^{-10}

SUMMARY

CRYSTAL BOX (PRELIMINARY) 90% C.L.s

$$^{\bullet} \quad B(\mu \rightarrow e \gamma) < 1.4 \times 10^{-10}$$

$$^{\bullet\bullet} \quad B(\mu \rightarrow e \gamma \gamma) < 3.8 \times 10^{-10}$$

$$^{\bullet\bullet} \quad B(\mu \rightarrow e e e) < 1.3 \times 10^{-10}$$

No evidence for nonconservation of
separate family numbers in muon decay

$^{\bullet}$ Based on 0.97×10^{11} muon stops

$^{\bullet}$ Based on 2.20×10^{11} muon stops

Total number of muon stops in final data = 9.5×10^{11}

Expect a final sensitivity of a few $\times 10^{-11}$